Damage Localization and Quantification of Earthquake Excited RC-Frames

Skjærbæk, P. S.; Nielsen, Søren R. K.; Kirkegaard, Poul Henning; Cakmak, A. S.

Published in:
Earthquake Engineering and Structural Dynamics

DOI (link to publication from Publisher):
10.1002/(SICI)1096-9845(199809)27:9<903::AID-EQE757>3.0.CO;2-C

Publication date:
1998

Document Version
Publisher's PDF, also known as Version of record

EARTHQUAKE ENGINEERING AND STRUCTURAL DYNAMICS
Earthquake Engng. Struct. Dyn. **27**, 903–916 (1998)

DAMAGE LOCALIZATION AND QUANTIFICATION OF EARTHQUAKE EXCITED RC-FRAMES

P. S. SKJÆRBÆK[1,*], S R. K. NIELSEN[1], P. H. KIRKEGAARD[1] AND A. Ş. ÇAKMAK[2]

[1] *Department of Building Technology and Structural Engineering, Aalborg Univrsity, DK-9000 Aalborg, Denmark*
[2] *Department of Civil Engineering and Operations Research, Princeton University, Princeton, NJ 08544, U.S.A.*

SUMMARY

In the paper a recently proposed method for damage localization and quantification of RC-structures from response measurements is tested on experimental data. The method investigated requires at least one response measurement along the structures and the ground surface acceleration. Further, the two lowest time-varying eigenfrequencies of the structure must be identified. The data considered are sampled from a series of three RC-frame model tests performed at the structural laboratory at Aalborg University, Denmark during the autumn of 1996. The frames in the test series were exposed to two or three series of ground motions of increasing magnitude. After each of these runs the damage state of the frame was examined and each storey of the frame were classified into one of the following six classifications: undamaged, cracked, lightly damaged, damaged, severely damaged or collapse. During each of the ground motion events the storey accelerations were measured by accelerometers. After application of the last earthquake sequence to the structure the frames were cut into pieces and each of the beams and columns was statically tested and damage assessment was performed using the obtained stiffnesses. The damage in the storeys determined by the suggested method was then compared to the damage classification from the visual inspection as well as the static tests. It was found that especially in the cases where the damage is concentrated in a certain area of the structure a very good damage assessment is obtained using the suggested method. © 1998 John Wiley & Sons, Ltd.

KEY WORDS: RC-frames; shaking table testing; response measurements; damage

1. INTRODUCTION

During the last 2–3 decades a high number of damaging seismic events have shown a growing need for methods for localization and quantification of damage evolved in Reinforced Concrete (RC) structures during earthquakes. As a consequence, a lot of research work has been invested in the development of methods for assessment of damage in RC-structures that have been subjected to an earthquake. Due to the lack of instrumentation of structures in the early days of earthquake engineering, the initial research was concentrated on assessment of the damage from visual inspection simply by measuring crack widths, permanent deformations, etc. Such an investigation of an entire building may be very cumbersome, since all panels and other things covering the bearing structural elements necessarily must be removed. Such a process is obviously very time consuming and can be critical for buildings of major social and economical importance such as hospitals, etc. The rapid advance during the last 2 decads in digital technology, the horizon for a much more feasible approach, using response measurements has opened. Since the late 1970s several methods for assessment of damage in RC-frames from measurement of storey responses have been suggested.

* Correspondence to: P. S. Skjærbæk, Department of Building Technology and Structural Engineering, Aalborg University, Sohngaardsholmsvej 57, 9000 Aalborg, Denmark

Contract/grant sponsor: Danish Technical Research Council

CCC 0098–8847/98/090903–14$17·50

Received 25 August 1997
Revised 27 January 1998

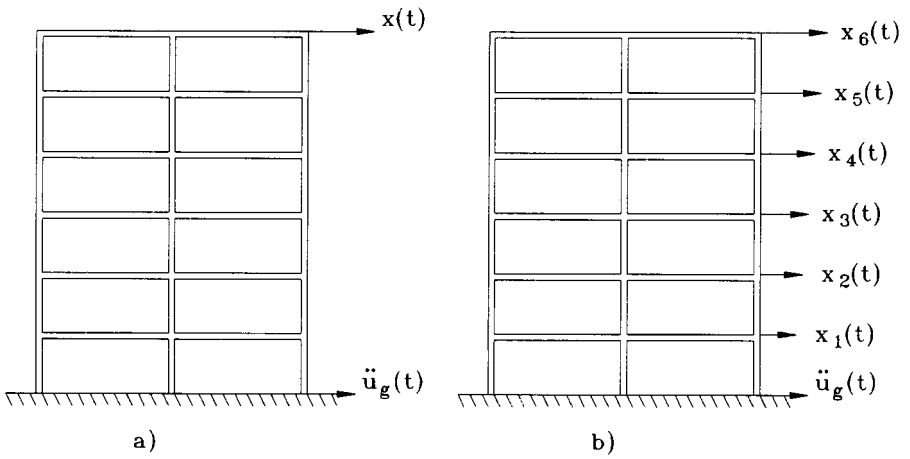

Figure 1. (a) Instrumentation required for the local softening damage index. (b) Instrumentation at all storeys required by traditional indicators

Culver *et al.*,[1] Toussi and Yao,[2] and Sozen[3] all suggested different kinds of damage indices based on measured interstorey drifts. Banon *et al.*[4] considered different indices such as flexural damage ratios, normalized cumulative rotations and normalized cumulative energy. Yao and Munze[5] and Stephens and Yao[6] formulated damage indices based on low-cycle fatigue. Park and Ang[7] suggested a damage index calculated as a combination of a maximum displacement term and a cumulative dissipated energy term. However, in order to obtain an assessment of damage in each of the storeys of an RC-frame, all the mentioned damage indices require response measurements at each storey building. Many of the structures instrumented today do not have such an extensive instrumentation, but merely a measurement at the base and at the top storey of the building. Skjærbæk *et al.*[8] suggested a local softening damage index with due consideration to this fact. This index is calculated from identified time-varying eigenfrequencies of the structure which can normally be extracted from a single-response measurement.

The purpose of this paper is to investigate and evaluate this local softening damage index on a series of shaking table tests with three, two-bay, six-storey model test RC-frames, scale 1·5. During the tests the frames are instrumented with accelerometers at the base and at the top storey as illustrated in Figure 1(a). Each frame is subjected to two or three sequential series of ground motions of increasing magnitudes. After each of these series a thorough visual inspection of the frame is performed and it is investigated how well the calculated local softening damage index reflects the observed damage state of the frame. Further, static tests are performed with parts of the structure to investigate which parts show the largest loss of stiffness. The damage indicators based on these static tests are used as a reference for the validation of the proposed damage localization method.

2. PROPOSED LOCALIZATION PROCEDURE

In principle, the identification of the structural damage by the proposed method (LSDI), see Reference 8, consists of two main phases:

1. Analysis of available records and estimation of the time varying two lowest eigenfrequencies.
2. Evaluation of structural parameters by means of a substructure technique with a least-squares approach using the determined modal quantities from phase 1.

When an RC-structure are subjected to strong ground motions the modal parameters will show heavy fluctuations as the structure enters and leaves the plastic regime. Obviously, these heavy fluctuations cannot be extracted from measured storey accelerations and only the long-term development can be extracted. This long-term development of the modal parameters will be referred to as smoothed values.

Estimation of smoothed modal parameters from strong motion records has been dealt within several papers, see e.g. References 9 and 10. Within this study a recursive implemented AutoRegressive Moving-Average model (ARMA) has been used and the following derivations will be concentrated on solving phase 2.

It is assumed that a linear finite element model of the undamaged structure is available. In case of free vibrations where the structure remains in the linear elastic range, the motion is described by the following equation:

$$\mathbf{M}\ddot{\mathbf{x}}(t) + \mathbf{K}_0\mathbf{x}(t) = \mathbf{0} \tag{1}$$

where $\mathbf{M}$ is the mass matrix, $\mathbf{K}_0$ is the undamaged stiffness matrix and $\mathbf{x}(t)$ is an n-dimensional vector of displacements and rotations of the structure.

The corresponding modal quantities, circular eigenfrequencies $\omega_{i,0}$ and mode shapes $\mathbf{\Phi}_{i,0}$ of such a linear undamaged structure are determined from the eigenvalue problem

$$(\mathbf{K}_0 - \omega_{i,0}^2\mathbf{M})\mathbf{\Phi}_{i,0} = \mathbf{0} \tag{2}$$

During a strong motion earthquake, the initial stiffness matrix $\mathbf{K}_0$ will start changing, causing changes in the modal parameters. These are the parameters that can be 'measured' through earthquake excitations. Then, the task is to solve this inverse problem of determining the time-varying elements in the stiffness matrix from the measured modal quantities. Normally, this set of equations is underdetermined due to limited numbers of observations, and the limited number of modes activated, and therefore it requires special techniques to be solved.

The present damage localization method is based on a sequence of substructurings in which the damage in each substructure is sequentially estimated. At the first level, the structure is divided into two substructures labelled 1 and 2 as illustrated in Figure 2(a). Then

$$\mathbf{K}_0 = \mathbf{K}_{1,0}^{(1)} + \mathbf{K}_{2,0}^{(1)} \tag{3}$$

where $\mathbf{K}_{1,0}^{(1)}$ and $\mathbf{K}_{2,0}^{(1)}$ signify the global undamaged stiffness matrices of substructures 1 and 2. Although $\mathbf{K}_0$ is positive definite its constituents $\mathbf{K}_{1,0}^{(1)}$ and $\mathbf{K}_{2,0}^{(1)}$ are both positive semi-definite, i.e. they contain a large number of zero components corresponding to the global positions of the extracted substructure. The subscripts 1 and 2 refer to substructures 1 and 2, and the subscript 0 refers to the initial state. The superscript (1) refers to the first level of substructuring.

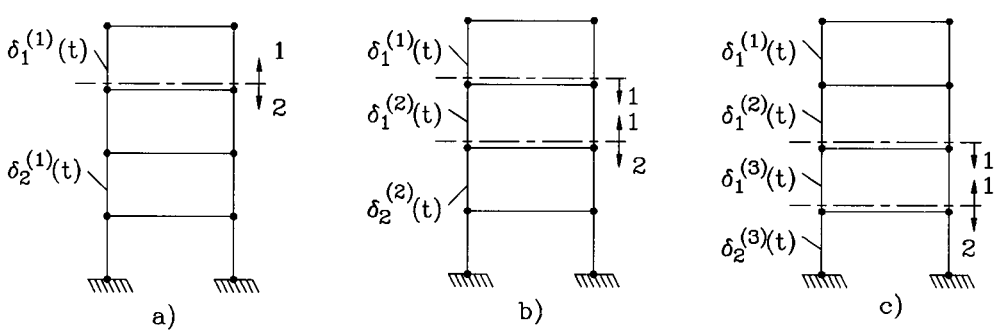

Figure 2. Possible procedure for changing the sequence of substructuring for a 1-bay, four-storey frame

Next, a stiffness matrix $\mathbf{K}_e(t)$ for the equivalent linear structure can be defined in the following way:

$$\mathbf{K}_e^{(1)}(t) = (1 - \delta_1^{(1)}(t))^2 \mathbf{K}_{1,0}^{(1)} + (1 - \delta_2^{(1)}(t))^2 \mathbf{K}_{2,0}^{(1)} \tag{4}$$

where $\delta_1^{(1)}(t)$ and $\delta_2^{(1)}(t)$ signify the damage indices for substructures 1 and 2, respectively. These may be interpreted as measures of the average stiffness losses in the substructure. It should be noted here, that when only one substructure is used, the corresponding damage measure $\delta_1(t)$ is equivalent to the so-called global softening index defined by DiPasquale and Çakmak.[11]

Next, $\delta_1^{(1)}(t)$ and $\delta_2^{(1)}(t)$ are identified so that $\mathbf{K}_e^{(1)}(t)$ as given by equation (4) provides the smoothed measured eigenfrequencies $\langle \omega_i(t) \rangle$ identified from the available records, i.e.

$$\left(\sum_{j=1}^{2} (1 - \delta_j^{(1)}(t))^2 \mathbf{K}_{j,0}^{(1)} - \langle \omega_i(t) \rangle^2 \mathbf{M} \right) \mathbf{\Phi}_i(t) = \mathbf{0} \tag{5}$$

where $\mathbf{\Phi}_i(t)$ are the ith mode shape of the equivalent structure.

The time-varying equivalent linear stiffness matrix of substructure 1 is then estimated as $(1 - \delta_1^{(1)}(t))^2 \mathbf{K}_{1,0}^{(1)}$. Next, the previously labelled substructure 2 can be divided into two new substructures, again labelled 1 and 2. Then, a new stiffness matrix of the equivalent linear structure can be written on the form

$$\mathbf{K}_e^{(2)}(t) = (1 - \delta_1^{(1)}(t))^2 \mathbf{K}_{1,0}^{(1)} + (1 - \delta_1^{(2)}(t))^2 \mathbf{K}_{1,0}^{(2)} + (1 - \delta_2^{(2)}(t))^2 \mathbf{K}_{2,0}^{(2)} \tag{6}$$

where

$$\mathbf{K}_{2,0}^{(1)} = \mathbf{K}_{1,0}^{(2)} + \mathbf{K}_{2,0}^{(2)} \tag{7}$$

Since $\delta_1^{(1)}(t)$ is known, $\delta_1^{(2)}(t)$ and $\delta_2^{(2)}(t)$ can be estimated, inserting equation (6) into equation (5). From a new system identification, $\delta_1^{(2)}(t)$ and $\delta_2^{(2)}(t)$ are then obtained.

The procedure of dividing the previously labelled substructure 2 into two new substructures can be repeated further. Assuming that this procedure has been performed i times the stiffness matrix of the equivalent linear system can be written as

$$\mathbf{K}_e^{(i)}(t) = \sum_{j=1}^{i-1} (1 - \delta_1^{(j)}(t))^2 \mathbf{K}_{1,0}^{(j)} + (1 - \delta_1^{(i)}(t))^2 \mathbf{K}_{1,0}^{(i)} + (1 - \delta_2^{(i)}(t))^2 \mathbf{K}_{2,0}^{(i)} \tag{8}$$

where equation (4) corresponds to $i = 1$ and equation (6) to $i = 2$.

In equation (8) $\delta_1^{(1)}(t), \ldots, \delta_1^{(i-1)}(t)$ is known from previous identifications. $\delta_1^{(i)}(t)$ and $\delta_2^{(i)}(t)$ can then be identified by inserting equation (8) into equation (5). Below, all the contributions to the stiffness from previous levels of substructuring, i.e. the summation $\sum_{j=1}^{i-1} (1 - \delta_1^{(j)}(t))^2 \mathbf{K}_{1,0}^{(j)}$, will be referred to as $\mathbf{K}_{0,0}^{(i)}$ for convenience of notation.

By applying the above procedure with substructuring at storey level, $\delta_1^{(i)}(t)$ provides a measure of the average damage of each storey. If further localization within a given storey needs to be performed, it can, in principle, be done by further substructuring within the said storey. When using the method it should be kept in mind that symmetrically placed elements in a symmetric structure will cause the same change in eigenfrequencies and mode-shape components, and the localization is therefore limited to one of two possibilities. This limitation is illustrated in Figure 3 where it is seen that the damage scenarios illustrated in the figure to the left will give the same changes in eigenfrequencies and mode-shape components as the scenarios shown to the right.

3. IDENTIFICATION OF LOCAL SOFTENING DAMAGE INDICES (LSDI)

Initially, the eigenvalue problem (2) is solved by means of a subspace iteration yielding the two lowest circular eigenfrequencies $\omega_{1,0}\omega_{2,0}$ and the corresponding mode shapes $\mathbf{\Phi}_{1,0}$ and $\mathbf{\Phi}_{2,0}$ of the undamaged structure.

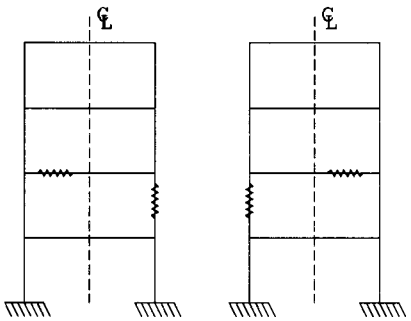

Figure 3. Example of damage scenarios giving the same changes in eigenfrequencies and horizontal mode-shape components for a one-bay, four-storey frame

A first estimate of the damage indices at the time t can be obtained using a Rayleigh fraction where the time-averaged circular eigenfrequencies at the time t and the mode shapes of the undamaged structure are applied. Based on the damage indices $\delta^{(i)}_{1,1}(t)$, $\delta^{(i)}_{2,1}(t)$ thus determined, new mode shapes can be determined as eigenvectors to $(\mathbf{K}_e(\delta^{(i)}_{1,1}, \delta^{(i)}_{2,1}) - \langle\omega_j(t)\rangle^2\mathbf{M})$. These new mode shapes are then used in the Rayleigh fraction and better local damage indices are obtained . This procedure is repeated until a stable solution is found. The values of at the nth step of this iteration process are designated $\delta^{(i)}_{1,n}(t), \delta^{(i)}_{2,n}(t)$, where the formulas look as follows:

$$\langle\omega_j(t)\rangle^2 = \frac{\mathbf{\Phi}^{\mathrm{T}}_{j,n-1}\mathbf{K}_e(\delta^{(i)}_{1,n}(t),\delta^{(i)}_{2,n}(t))\mathbf{\Phi}_{j,n-1}}{\mathbf{\Phi}^{\mathrm{T}}_{j,n-1}\mathbf{M}\mathbf{\Phi}^{\mathrm{T}}_{j,n-1}}, \quad j = 1,2,\ n = 1,2,\ \ldots \tag{9}$$

$\mathbf{\Phi}_{j,n-1} = \mathbf{\Phi}_{j,n-1}(t)$ are the mode shapes calculated at the $(n-1)$th step of iteration, i.e. corresponding to the stiffness matrix $\mathbf{K}_e(\delta^{(i)}_{1,n-1}(t),\delta^{(i)}_{2,n-1}(t))$. Insertion of the definition of $\mathbf{K}_e(\delta^{(i)}_{1,n}(t),\delta^{(i)}_{2,n}(t))$ given by equation (9) into equation (9) provides the following two linear equations in $(1-\delta^{(i)}_{1,n}(t))^2$ and $(1-\delta^{(i)}_{2,n}(t))^2$ for the determination of damage measures of the nth iteration step:

$$\langle\omega_j(t)\rangle^2 = \frac{\mathbf{\Phi}^{\mathrm{T}}_{j,n-1}\mathbf{K}^{(i)}_{1,0}(1-\delta^{(i)}_{1,n}(t))^2\mathbf{\Phi}_{j,n-1} + \mathbf{\Phi}^{\mathrm{T}}_{j,n-1}\mathbf{K}^{(i)}_{2,0}(1-\delta^{(i)}_{2,n}(t))^2\mathbf{\Phi}_{j,n-1}}{\mathbf{\Phi}^{\mathrm{T}}_{j,n-1}\mathbf{M}\mathbf{\Phi}_{j,n-1}}$$

$$+ \frac{\mathbf{\Phi}^{\mathrm{T}}_{j,n-1}\mathbf{K}^{(i)}_{0,0}\mathbf{\Phi}_{j,n-1}}{\mathbf{\Phi}^{\mathrm{T}}_{j,n-1}\mathbf{M}\mathbf{\Phi}_{j,n-1}}, \quad j = 1,2 \tag{10}$$

From the determined values of the local damage indices $\delta^{(i)}_{1,n}(t), \delta^{(i)}_{2,n}(t)$, a new equivalent stiffness matrix can be calculated. The corresponding new eigenmodes $\mathbf{\Phi}_{1,n}, \mathbf{\Phi}_{2,n}$ can be found from

$$(\mathbf{K}^{(i)}_e(\delta^{(i)}_{1,n}(t),\delta^{(i)}_{2,n}(t)) - \langle\omega_i(t)\rangle^2\mathbf{M}_0)\mathbf{\Phi}_{i,n} = \mathbf{0} \tag{11}$$

This procedure, equations (9)–(11), is repeated at each level of substructuring until no change occurs in the local damage index, i.e. $|\delta^{(i)}_{1,n} - \delta^{(i)}_{1,n-1}| + |\delta^{(i)}_{2,n} - \delta^{(i)}_{2,n-1}| < \varepsilon$, where ε is a tolerance of the magnitude 10^{-5}.

4. EXPERIMENTAL RESULTS

The data considered in this paper were sampled from a total of three identical model test RC-frames (scale 1:5) tested at the Structural Laboratory at Aalborg University, Denmark during the autumn of 1996).

4.1. Description of the tests

The tests were conducted as shaking table tests and a photo of the test set-up is shown in Figure 4(a).

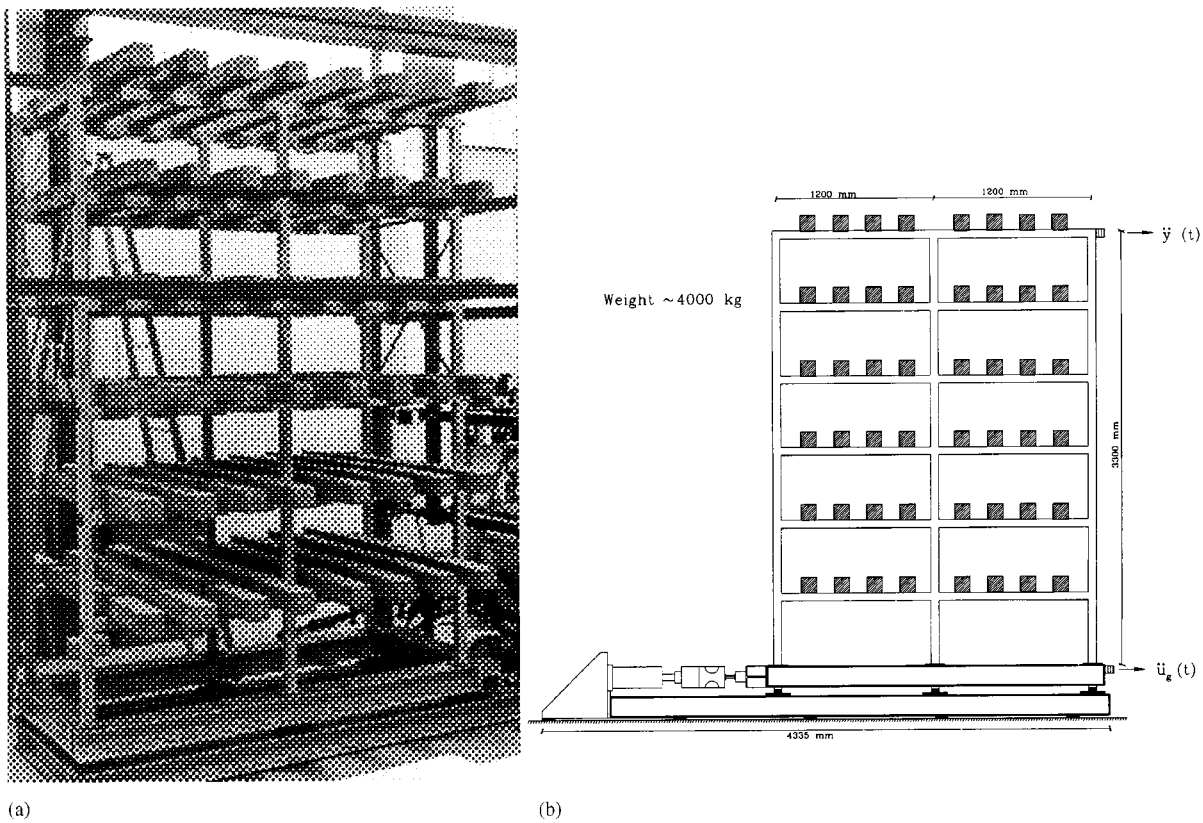

Figure 4. (a) Photo of the test set-up. (b) Side view of experimental set-up

As seen from Figure 4(a) the frames were tested in pairs of two, where the storey weights are modelled by placing RC-beams in span between the two frames. Each of the two frames was instrumented with a Brüel and Kjær accelerometer at the top storey and at the base to measure the ground motions. The force was provided by a 63 kN HBM cylinder with a stroke of $\pm$ 20 mm. In Figure 4(b) a schematic view of the test set-up is shown.

The frames were cast *in situ* and consist of beams and columns with cross-sections of 50×60 mm. The beams were reinforced with 4ø6 KS410 ribbed steel bars with an average yield strength of 600 MPa. The concrete used had a strength of 20 MPa. The columns were reinforced with six reinforcement bars of the same type as in the beams. In Figure 5 the cross-sections of the beams and columns are shown.

The storey height is 0·55 m giving the model a total height of 3·3 m. Each of the two bays is 1·2 m wide giving the model a total width of 2·4 m. At each storey 8 $0{\cdot}12 \times 0{\cdot}12 \times 2$ m RC-beams are placed between the two parallel frames to model the storey weights giving the model a total weight of approximately 40 kN.

During the tests two types of ground motion labelled a and b were applied. The type a ground motion had the dominant frequency chosen close to the first eigenfrequency of the undamaged test structure and a type b ground motion had the dominant frequency close to the second eigenfrequency of the undamaged test structures. The realizations of these ground motions were obtained by filtering amplitude modulated Gaussian white noise through a Kanai–Tajimi filter.[12] Each of the ground motion series had a length of 20 s. The applied ground motions are shown in Figure 6.

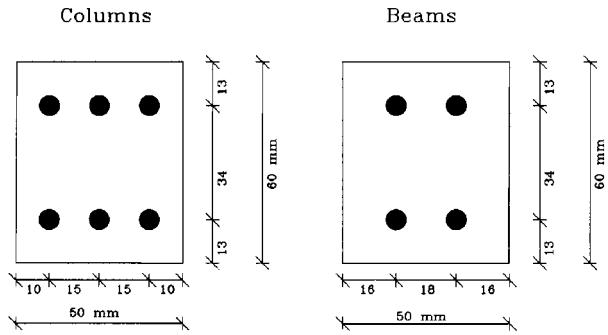

Figure 5. Cross-section of beam and columns

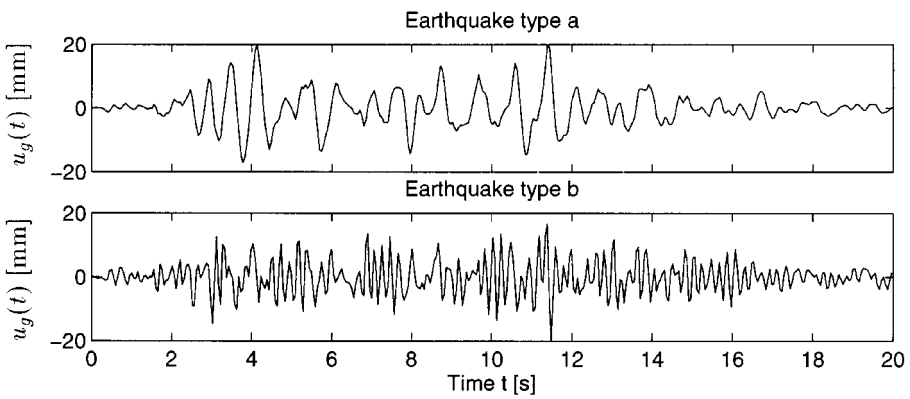

Figure 6. Displacements $u_g(t)$ of applied earthquake types scaled to maximum amplitude of 20 mm: (a) earthquake type a; (b) earthquake type b

In the following the three test set-ups will be labelled as AAU1, AAU2 and AAU3. The frame AAU1 was subjected to a sequence of three ground motions of type a illustrated in Figure 6(a) scaled with a factor of 0·25, 0·50 and 0·75, respectively. The frame AAU2 was subjected to a sequence of two ground motions of type a scaled with a factor of 0·2 and 0·4. Finally, the frame AAU3 was subjected to a sequence of three ground motions of type b scaled with a factor of 0·1, 0·2 and 0·35, respectively.

4.2. Observed damage from visual inspection

The classifications defined in Table I were used for the damage assessment based on visual inspection.

4.2.1. Results of visual inspection of frame AAU1. The visual damage assessment for frame AAU1 after each of the three ground motions is shown in Table II.

As indicated in Table II only a few cracks were found in the structure after the first earthquake. The cracks were concentrated at the joints between columns and beams in the second storey. At the remaining storeys smaller cracks were found. After the second earthquake extensive crack growth was observed in the lower part of the frame and localized crushing of concrete had taken place at the centre node in the first and second storey. During the third earthquake damage developed dramatically in the second storey and after approximately 10 s of excitation the second storey collapsed. Here it should be noted that although the third storey

Table I. Definition of the six damage classifications used

Category	Definition
Undamaged **UD**	No external sign of changed integrity of any of the columns or beams in the storey
Cracked **CR**	Light cracking observed in several members but no permanent deformation
Lightly damage **LD**	Severe cracking observed with minor permaent deformations
Damaged **D**	Severe cracking and local permanent deformations observed
Severe damage **SD**	Large permanent deformation observed and spalling of concrete at some members
Collapse **CO**	Very large permanent deformations observed and severe spalling of concrete at several members

Table II. Damage classifications after the three earthquake events for frame AAU1

Storey	EQ1	EQ2	EQ3
1st	**UD**	**CR**	**SD**
2nd	**CR**	**LD**	**CO**
3rd	**CR**	**LD**	**CO**
4th	**UD**	**CR**	**LD**
5th	**UD**	**CR**	**CR**
6th	**UD**	**RC**	**CR**

Table III. Damage classifications after the two earthquake events for frame AAU2

Storey	EQ1	EQ2
1st	**CR**	**D**
2nd	**CR**	**D**
3rd	**CR**	**LD**
4th	**UD**	**CR**
5th	**UD**	**CR**
6th	**CR**	**CR**

has been assessed as collapsed after EQ3 this may not have been caused by the strong motions during EQ3, but merely by the impact when structural parts above the second storey fell one storey down during the collapse.

4.2.2. Results of visual inspection of frame AAU2. Visual damage assessment of frame AAU2 was performed after EQ1 and EQ2. The results are shown in Table III.

Before the strong motion testing the structure was examined and shear cracks were found in the beam at the first, third and sixth storey. These were caused by the handling of the frames during the construction phase.

After the first earthquake only a limited amount of microcracks were observed at the three lower storeys and at the top storey. The cracks were largest and most dense at the nodes of the first and second storey. At the remaining storeys only small cracks were found. After the second earthquake extensive crack growth was observed in the lower part of the frame and localized crushing of concrete at the centre node in the first and second storey was observed. Besides, shear cracks had been generated at the nodes in the third storey and in the beam at the top storey and already existing cracks had become longer.

4.2.3. Results of visual inspection of frame AAU3. Before the strong motion testing the structure was examined and shear cracks were found in the beams at the first and sixth storey (Table IV). After the first earthquake only microcracks were observed at the three lower storeys and at the top storey. The cracks were largest and most dense in the nodes at the third, fourth and fifth storey. At the remaining storeys generally only small cracks were found. After the second earthquake extensive crack growth was observed at the nodes in the fourth and fifth storeys. Furthermore, several shear cuts (horizontal cracks) were observed in the columns at the third, fourth and fifth storey. After the third earthquake crack growth was observed in all storeys and, furthermore, crushing of concrete was seen at the centre column node in the first, fourth and fifth storey.

4.3. Estimated damage from static tests

After the last application of strong motion one of the two frames of AAU2 and AAU3 was cut into smaller pieces by dividing each beam and column in to halves. The cutting was performed using a high-speed diamond-based cutting device. Half-beams and columns were subjected to a static test where a force was applied at the end of the beam or column. The corresponding values of force and displacement were sampled for forces in the range of 0·0–1·0 kN for the columns and in the range of 0·0–0·4 kN for the beams. A schematic view of the test set-up is shown in Figure 7(a).

Based on the static tests performed with each of the beams and columns the lateral stiffness can be estimated. In the following investigations only the initial tangent stiffness k_i of the obtained force–deformation curves of beams and columns is considered, see Figure 7(b).

As reference an undamaged frame was undergoing the same process of cutting and static testing to evaluate the corresponding undamaged initial stiffness $k_{i,0}$ for the beams and columns, see Figure 7b.

A damage index for beam or column no. i can then be defined as

$$\mathrm{ST}_i = 1 - \sqrt{\frac{k_i}{k_{i,0}}} \tag{12}$$

Table IV. Damage classifications after the three earthquake events for frame AAU3

Storey	EQ1	EQ2	EQ3
1st	**CR**	**LD**	**D**
2nd	**CR**	**D**	**D**
3rd	**CR**	**LD**	**LD**
4th	**CR**	**LD**	**D**
5th	**CR**	**LD**	**D**
6th	**CR**	**CR**	**CR**

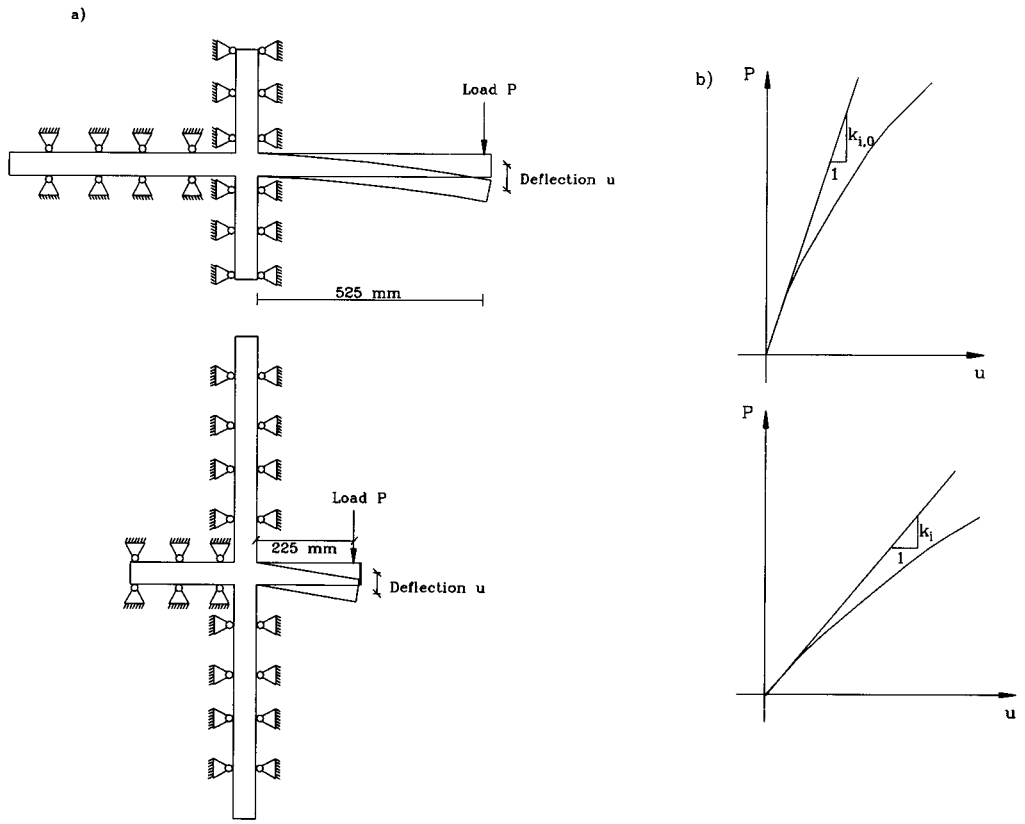

Figure 7. (a) Schematic view of the test set-up used for the static testing of beams and columns. (b) Definition of initial stiffness of undamaged and damaged specimen

Next, each of the half-beam damage indices is weighted into one-storey damage index using the following method by Park *et al.*:[13]

$$\mathrm{ST_g} = \frac{\sum_{i=1}^{n} \mathrm{ST}_i^2}{\sum_{i=1}^{n} \mathrm{ST}_i} \tag{13}$$

where n is the number of elements in each storey. Since no unique mapping of local damage indices into global one exists, equation (13) is the only one of multiple possible weights that can be used to calculate a global damage index from local damage indices. The weights could also be assigned from considerations such as lower storeys are more important than upper storeys, columns are more important than beams, etc.

It should be noted that the damage index ST_i is consistent with the formulation used for the local softening damage indicator. The ST_i damage index and the related storey damage indicktor $\mathrm{ST_g}$ are considered as the 'true' measure of damage and the damage predictions of Section 3 are evaluated relative to this. The following storey damage indicators given in Table V were obtained from static testing of frames AAU2 and AAU3.

In case of frame AAU3 a completely different damage pattern is obtained compared to AAU2. It is seen that the fourth and fifth storeys were the most damaged, followed by the first and second storeys, whereas the third and sixth storey suffered the least damaged.

Table V. Storey damage indices evaluated from static tests after the final series of strong motion

	Storey					
	1st	2nd	3rd	4th	5th	6th
AAU2	0·27	0·31	0·25	0·24	0·22	0·22
AAU3	0·30	0·30	0·26	0·35	0·33	0·24

Table VI. Estimated LSDIs for each storey in frame AAU1 after EQ1, EQ2 and EQ3

	Storey					
Case	1st	2nd	3rd	4th	5th	6th
EQ1	0·32	0·33	0·31	0·00	0·00	0·00
EQ2	0·52	0·41	0·34	0·00	0·00	0·00
EQ3	0·62	0·64	0·34	0·00	0·00	0·00

4.4. Estimated damage from response measurements

After application of each of the strong motions the development in the two lowest smoothed eigenfrequencies of the structure was extracted using a Recursive–AutoRegressive Moving-Average model (RARMA) and the local softening index defined in Section 2 was calculated at the time where the maximum reduction in the first smoothed eigenfrequency was observed. The estimation method for extracting the smoothed eigenfrequencies has been thoroughly described in Skjærbæk.[14]

4.4.1. Damage assessment of frame AAU1. From series of smoothed eigenfrequencies extracted from the measured top storey acceleration during the strong motion events the LSDIs listed in Table VI were evaluated at the time where the maximum reduction of the first eigenfrequency was observed.

As seen in Table VI, a relatively high-damage level is observed already after EQ1 in the lower storeys, whereas the three upper storeys are undamaged. During the second earthquake damage is seen to increase in the lower-half of the structure. The growth of damage is primarily in the first and second storeys. During EQ3 a large growth in the damage is observed in the second storey. This prediction by the LSDI method is in very good agreement with the observations during EQ3 where the collapse actually occurred in the second storey.

4.4.2. Damage assessment of frame AAU2. As in the case of frame AAU1 the LSDIs were evaluated during the two strong motion events and the results are listed in Table VII.

From Table VII it is clear that damage is incurred mainly in the lower part of the frame during EQ1. In contrast to AAU1 a slight change in stiffness is seen in the upper storeys. This change is probably due to cracking of hitherto uncracked sections. Obviously, the stiffness changes from cracking will then appear as damage when the LSDI method is applied. During EQ2 the damage is seen to increase in the two lowest storeys and slightly also in the four upper storeys. Again the increase in the damage in the three upper storeys is most likely due to cracking.

4.4.3. Damage assessment of frame AAU3. The LSDI estimates in Table VIII indicate that the damage incurred in the frame AAU3 is much more uniformly distributed than is the case for the frames AAU1 and

Table VII. Estimated LSDIs for each storey in frame AAU2 after EQ1 and EQ2

	Storey					
Case	1st	2nd	3rd	4th	5th	6th
EQ1	0·22	0·22	0·21	0·07	0·06	0·06
EQ2	0·46	0·37	0·23	0·13	0·12	0·12

Table VIII. Estimated LSDIs for each storey in frame AAU3 after EQ1, EQ2 and EQ3

	Storey					
Case	1st	2nd	3rd	4th	5th	6th
EQ1	0·13	0·15	0·13	0·09	0·09	0·08
EQ2	0·24	0·26	0·24	0·18	0·18	0·16
EQ3	0·38	0·38	0·38	0·35	0·35	0·34

AAU2. As seen in general there is a tendency that the lower-half is slightly more damaged than the upper-half, but after EQ3 this tendency has diminished significantly and the LSDI basically predicts that all storeys on average are identically damaged.

5. DISCUSSION

Considering the damage assessment of frame AAU1 it is sen that the visual damage assessment and the LSDI provided somewhat similar results. However, even though the structure after the second strong motion event was in a moderate damage state, the visual inspection only indicated light damage of the structure. Alternatively, the LSDI method predicted the second storey to be the one with the highest damage level and therefore the storey likely to collapse. This highlights the limited reliability of visual inspection methods even under laboratory conditions. The tests with frame AAU1 indicate that the critical value of the LSDI is somewhere in the range of 0·6–0·7 for collapse of the substructure. This range of the LSDI corresponds to an average stiffness reduction of 75–90 per cent.

Comparing the two reference methods, visual inspection and static testing in the case of frame AAU2, it is seen that both methods clearly indicate the first and especially the second floor to be the most damaged. The third storey is found by both methods to be somewhat less damaged and finally the storeys 4–6 are found to be basically identically damaged. This general tendency is also given by the assessment obtained by the LSDI, which correctly pin points the two lowest storeys to be the most damaged ones.

As in the case of frame AAU2 the results from damage assessment of frame AAU3 show a good agreement between the damage assessment obtained by the static testing and the visual inspections. Both methods indicate a uniformly distributed damage with slightly higher-damage level in the first, second, fourth and fifth storeys. The static testing indicated a slightly higher-damage level in the fourth and fifth storeys. Again the damage assessment by the LSDI correctly displayed the damage distribution.

When comparing the LSDI and the static testing it should be noted that the LSDI is based on an average force–determination relationship obtained under cyclic loading which may be more representative of

a peak-to-peak equivalent stiffness of the largest hysteretic load which differs from the static force–deformation relationship. This subject is discussed in, e.g. Reference 11.

Comparing the damage distributions of frame AAU1 and AAU2 some difference can be observed eventhough the same type of loadings have been used. This can be explained from the natural variations present in the concrete from inhomogeneities, etc. This was also displayed in the compression tests of the concrete where variations in strength and modulus of elasticity were found.

6. CONCLUSIONS

In this paper the results from damage assessment of three two-bay, six-storey, scale 1:5 model test frames have been presented. For each of the three frames different damage scenarios have been observed. The first frame AAU1 was subjected to three earthquake ground motions of increasing magnitude. The earthquakes were generated using a centre frequency close to the first eigenfrequency of the undamaged structure. Due to failure in the second storey the frame AAU1 collapsed during the third earthquake motion. The frame AAU2 was exposed to the same type of earthquake motion as frame AAU1. However, this frame was only subjected to two earthquake motions to ensure that the structure only suffered moderate damage and allow the structure to be statically tested afterwards. For the third frame AAU3 the centre frequency of the load process was changed to the vicinity of the second eigenfrequency of the undamaged frame AAU3.

The general conclusions from the investigations performed within this paper are that the local softening damage index seems to work very well in the cases where the structure was subjected to earthquake motions with centre frequencies close to the first mode of the structure due to the localized nature of the damage distribution in the structure. Especially in the case where the structure was tested all the way up to failure, the local softening damage index was found to predict the damage growth in the failing storey very well. In the case of frame AAU3 the visual inspection and the damage assessment based on static testing revealed that the damage in the structure was more uniformly distributed than in the case of AAU1 and AAU2. Only the third and sixth storeys were found to be significantly less damaged than the rest of the structure. In this case the damage assessment by the local softening damage index predicted a somewhat uniformly distributed damage in the structure.

ACKNOWLEDGEMENTS

The present research was partially supported by The Danish Technical Research Council within the project: *Dynamics of Structures.*

REFERENCES

1. C. G. Culver *et al.*, 'Natural hazards evaluation of existing buildings', *Report No. BSS61*, National Bureau of Standards, U.S. Department of Commerce, 1975.
2. S. Toussi, J. P. T. Yao, 'Assessment of damage using the theory of evidence', in *Structural Safety*, Vol. 1, Elsevier, Amsterdam, Netherlands, 1982, pp. 107–121.
3. M. A. Sozen, 'Review of earthquake response of reinforced concrete buildings with a view to deift control', *State-of-the-art-in-Earthquake-Engineering*, 1981, Turkish National Committee on Earthquake Engineering, Istanbul, Turkey, pp. 383–418.
4. H. Banon and D. Veneziano, 'Seismic safety of reinforced concrete members and structures, *Earthquake Engng. Struct. Dyn.* **10**, 179–193 (1982).
5. J. P. T. Yao and W. Munse, 'Low cycle axial fatigue behaviour of mild steel', *ASTM Special Publication, No. 338*, 1968, pp. 5–24.
6. J. E. Stephens and J. P T. Yao, 'Damage assessment using response measurements', *ASCE J. Struct. Engng* **113**(4), 787–801 (1987).
7. Y. J. Park, A. H.-S. Ang, 'Mechanistic seismic damage model for reinforced concrete', *ASCE J. Struct. Engng.* **111**(4), 722–739 (1985).
8. P. S. Skjærbæk, S. R. K. Nielsen and A. S. Çakmak, 'Assessment of damage in seismically excited RC-structures from a single measured response', *Proc. 14th IMAC*, Dearborn, MI, U.S.A., 12–15 February, 1996, pp. 133–139.
9. C. Mullen, R. C. Micaletti and A. Ş. Çakmak, 'A simple method for estimating the maximum softening damage index', *Proc. 7th Int. Conf. on Soil Dynamics and Structural Engineering*, 24–26 May 1995, Chania, Crete, Greece, pp. 371–378.

10. P. H. Kirkegaard, P. S. Skjærbæk and P. Andersen, 'Identification of timevarying civil engineering structures using multivariate recursive time domain models', *Proc. 21st ISMA*, Leuven, Belgium, 18–20, September 1996.
11. E. DiPasquale and A. Ş. Çakmak, 'Seismic damage assessment using linear models', *Soil Dyn. Earthquake Engng.* **9**(4), 194–215 (1990).
12. H. Tajimi, 'Semi-empirical formula for the seismic characteristics of the ground', *Proc. 2nd World Conf. on Earthquake Engineering*, Vol. II, Tokyo, Kyoto, 1960, pp. 781–798.
13. Y. J. Park, A. H.-S. Ang and Y. K. Wen, 'Seismic damage analysis of reinforced concrete buildings', *ASCE J. Struct. Engng.* **111**(4), 740–757 (1985).
14. P. S. Skjærbæk, 'Response and damage assessment of reinforced concrete frames subject to earthquakes', *Ph.D. Thesis*, Aalborg University, Denmark, June 1997.

